INSTITUTO DE INGENIEROS DE MINAS DEL PERÚ

proEXPLO 2019

Links between organic matter and gold-bearing arsenian pyrite at Shahuindo (Cajamarca, Peru): an integrated analytical and modeling study

Jean Vallance[1], Macneill Balboa [1], Brigitte Berna [1], Omar Cabrera [2] Camille Baya [3], Patrice Baby [3], Gleb S. Pokrovski [3]

[1] Especialidad Ingeniería Geológica, Pontificia Universidad Católica del Perú, Av. Universitaria 1801, San Miguel, Lima, Peru (jvallance@pucp.pe)
[2] Tahoe Resources Peru S.A.C., Cal. Esquilache Nro. 371 Int. 1401 (Oficina 1401-B), San Isidro, Lima, Perú (Omar.Cabrera@tahoeresources.com)
[3] Géosciences Environnement Toulouse, Université de Toulouse, CNRS-IRD-OMP, 14 Av. E. Belin, F-31400 Toulouse, France (gleb.pokrovski@get.omp.eu)

1. Introduction

The spatial association of gold mineralization with carbonaceous pyrite-bearing rocks, with in places evidence of petroleum generation, is a ubiquitous feature of gold-rich systems such as Carlin-Type Gold Deposits (Cline et al., 2005), orogenic gold deposits (Large et al., 2011), and the famous Witwatersrand (Fuchs et al., 2016).

Despite this common association, little is known about the origin and mechanisms of transport and deposition of gold in the presence of organic matter. As a result, rather contradictory models involving carbon-rich rocks and sedimentary pyrite as the gold source (Large et al., 2011), reduction of gold by hydrocarbons and bitumen (Fuchs et al., 2016), have been proposed, in addition to the most commonly accepted theory that organic matter favors precipitation of gold from the fluid due to reducing conditions (e.g., Pokrovski et al., 2014 for review). Recent progress in sensitive in-situ methods such as LA-ICPMS, SIMS, HRTEM, XAS provides new data about gold redox and structural state (both metallic and structurally bound) and spatial distribution in Fe-As-S ore associated or not with organic matter (e.g., Reich et al., 2005). However, the ultimate causes of Au-C associations, the mechanisms of gold concentration in natural specific contexts and the timing of gold introduction yet remain subjects of hot debate.

In an attempt to address these important issues, we conducted an integrated study of mineralized samples from C-rich sandstone, siltstone, and shale rocks hosting the epithermal Shahuindo gold deposit, using a range of analytical techniques (optical and SEM), XRD, XRF, LA-ICPMS, AAS and ICP-AES), coupled with thermodynamic modeling of fluid-rock interactions in the given geological context. The results provide new insights into the temporal evolution of the ore-bearing hydrothermal system and reveal new, so far ignored, effects of carbonaceous matter on the formation of this and similar gold deposits.

2. Geological setting

The Shahuindo deposit is located 60 km southeast of the Cajamarca city in northern Peru within the Marañon Fold-Thrust Belt (MFTB). The

MFTB hosts the major porphyry, skarn and epithermal deposits of Central and Northern Peru (e.g. Noble and McKee, 1999; Scherrenberg et al., 2016). The Mesozoic MFTB sedimentary sequences are deformed by late Cretaceous-early Eocene thin-skinned thrust tectonics (Incaic orogen) and subsequent ore formation was likely caused by Oligocene to Miocene magmatism (Mégard, 1984; Benavides-Caceres, 1999; Eude, 2014; Scherrenberg et al., 2016). The sedimentary sequences in the vicinity of the Shahuindo mine were affected by folds and thrusts related to a décollement zone located within pyrite-bearing carbonaceous shale and siltstone rocks of the Chicama (Jurassic) and Santa Formations (early Cretaceous). Later NE-SW right-lateral tear faults slightly displaced the folds. Thrusts, fold axial plane and strike slip faults likely controlled the intrusions of andesitic to dacitic stocks during the Oligo-Miocene (26 to 16 Ma, zircons U-Pb dating, Bussey y Nelson, 2011).

3. Gold mineralization

3.1. Overview

Gold in the Shahuindo Mine is extracted by heap-leach methods from the Farrat early Cretaceous sandstone in the outcropping fold hinge of an anticline. The primary sulfide mineralization is preserved in the less permeable underlying Carhuaz formation and intrusive bodies, as well as in thrusts and NE-SW faults. The Shahuindo deposit has been interpreted as an intermediate-sulfidation system (Hodder, 2010; Defilippi et al., 2016). The major mineral assemblage consists of pyrite, pyrrhotite, arsenopyrite, chalcopyrite, sphalerite, tetrahedrite-tennantite, galena and traces of tellurobismuthite, stibnite, kobellite, boulangerite (Hodder, 2010; Defilippi et al., 2016; Vallance et al., 2018; this study). Gangue minerals comprise quartz, carbonates, white micas, pyrophyllite, kaolinite and aluminium phosphate-sulfate minerals (APS). No “visible” gold was detected by optical microscopy and SEM even in samples with grades up to 8 g/t Au. Bulk rock analyses of 4 representative samples show a positive correlation of Au with Fe, S and As and no correlation with C, Cu, Zn, Ag, Pb and Sb, suggesting that Au is likely to be hosted by iron sulfides and arsenides.

3.2. Ore mineralogy and pyrite chemistry

Pyrite is the most abundant sulfide at Shahuindo that precipitated during at least four stages, as inferred by textural analyses that reveal 4 distinct pyrite generations.

The earliest pyrite (py I) has framboidal texture and have grown in fine-grained sandstones and shales of the Chicama, Santa and Carhuaz Formations. Framboids range from 10 to 50 µm in size and show overgrowth with graphitic material. Framboids show a continuous transition to anhedral coarse pyrite crystals. This type of pyrite is not accompanied by other sulfide minerals and occurs as disseminations of regional extension strongly suggesting a diagenetic origin. Bulk rock analyses of C- and pyrite I-rich samples taken outside and within the deposit indicate no direct relationships between these parameters and gold content. LA-ICP-MS analyses of pyrite show As and Au contents up to 2,300 and 0.6 ppm, respectively (*Figure 1*).

Stage II pyrite (py II) was only observed in the deposit area with a particular spatial association with intrusive bodies. It occurs both in sedimentary rocks and intrusive bodies as subhedral to euhedral ≤0.5 mm disseminated crystals, in place forming aggregates or <5 mm veinlets infill. More exceptionally py II occurs as massive replacement in C-enriched sites, as breccia cement at the contact between intrusions and host rocks or in faults. Locally transition between py I and py II appears to be continuous as evidenced by direct nucleation of euhedral pyrite on framboids. Py II typically contains <50 µm blebs of pyrrhotite and pyrite abundance tends to increase with the organic matter content locally showing replacement of organic detritus and/or bioclasts. Arsenic contents of py II range from 5 to 6,500 ppm, and gold grades are up to 2 ppm.

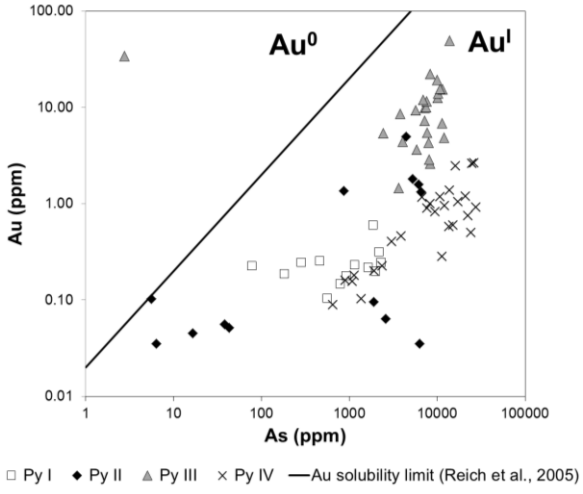

Figure 1. Distribution of As vs Au revealed by LA-ICPMS analyses for the four successive pyrite generations.

Arsenic- and gold-rich-pyrite (py III) occurs as rims and replacement zones on py II. This pyrite generation shows a complex zoning with As- and

mineral inclusion-rich bands (with chalcopyrite, arsenopyrite, sphalerite, galena, tetrahedrite-tennantite) alternating with As- and inclusion-poor growing zones. LA-ICPMS analyses of py III yield up to 2 wt% As and 50 ppm Au with a positive correlation between the two elements. Py III is also synchronous with the deposition of arsenopyrite with chalcopyrite, sphalerite, Bi-minerals, galena, stibnite and minor quartz and carbonates filling open spaces between arsenopyrite euhedral terminations. Tetrahedrite-tennantite shows crystal zoning as a result of fluctuation of the As/Sb ratio. Sphalerite shows also local zonation in its Fe-content. Our LA-ICPMS data demonstrate a close association between Au and As in arsenian pyrite (py III) from Shahuindo. Gold contents are below the saturation limit of metallic gold in arsenian pyrite proposed by Reich et al. (2005), thus suggesting that major part of Au is likely chemically bound in pyrite, in agreement with the apparent absence of gold visible particles.

The latest pyrite generation (py IV) occurs as rims on gold-rich pyrite py III and is generally inclusion-poor. It shows As contents similar to those of py III, but much lower gold contents (<3 ppm). This fourth generation of pyrite is accompanied by enargite and minor digenite replacing chalcopyrite. Gangue minerals include pyrophyllite, kaolinite and APS minerals (alunite, crandallite-florencite).

4. Thermodynamic modeling of gold transport and deposition

Quantitative modeling of Au incorporation in a chemically-bound form in pyrite and of the effect of arsenic in this process is currently hampered by a lack of direct data on gold chemical and thermodynamic state in pyrite. In contrast, good knowledge of Au speciation and solubility in hydrothermal fluids (e.g., Pokrovski et al., 2015) allow predictions of the evolution of gold metal saturation state in the fluid and examining different mechanisms of Au precipitation and the possible role of organic matter in these processes. We simulated interactions of an Au-bearing hydrothermal fluid and organic-bearing rocks in the context of the Shahuindo deposit. Gold was assumed to be transported by a low-salinity (5 wt% NaCl equivalent) S-bearing (sulfide+sulfate) acidic fluid (pH<5) of magmatic origin, in accord with the geological context of the region affected by strong magmatic influence. This fluid was interacted with a model hydrocarbon-bearing rock (C:H molal ratio ~2, fluid:rock ratio ~ 1:10 to 1:100) in the range 200-300°C, consistent with the temperatures inferred from the gangue mineral assemblages and a general epithermal-like setting of the deposit. The first results show that organic matter favors Au solubility in the form of Au(I) sulfide complexes, contrary to the common belief that hydrocarbons should lead to Au precipitation upon reduction. The key factor controlling Au solubility as identified by our quantitative modeling is the decrease in fluid acidity (i.e., pH) upon its interaction with hydrocarbon, leading to an increased solubility of the major Au bearing species in such fluids, $Au(HS)_2^-$, according to the reaction:

$$Au(s) + 2\ H_2S = Au(HS)_2^- + H^+ + 0.5H_2$$

The effect of pH increase (i.e., acidity or H^+ decrease) on Au solubility at our conditions is generally greater than or comparable to the opposite effect of redox on Au solubility. Thus, our first results indicate that organic matter may in some cases promote Au transport by hydrothermal fluids. This conclusion is in agreement with the paucity of Au in carbon-bearing rocks and framboidal sedimentary pyrite suggesting that Au-bearing fluids passed through organic sediments without losing much of its gold content. These fluids may have been trapped in favorable places of the deformed sedimentary sequence and precipitated gold and As-bearing pyrite together upon slow cooling, that is expected to have favored Au incorporation and enrichment in the pyrite structure in a bound state.

Thus, our model suggests a new, previously disregarded, mechanism of gold transport and deposition in carbon-rich sedimentary rocks.

5. Discussion and conclusions

Bulk rock and LA-ICPMS analyses performed in this work are in line with Tahoe geologists' observation (Wilder Garcia, personal communication) of the lack of a direct relationship between organic matter and pyrite-rich facies and gold grades. In particular, the LA-ICPMS analyses did not reveal the presence of an early Au-rich pyrite of regional distribution, which could be evoked as the metal source in a magmatism dominated context of the deposit.

The Shahuindo paragenetic sequence and mineral assemblages correspond to the lower limit of intermediate sulfidation states as suggested by the presence of arsenopyrite, chalcopyrite, tetrahedrite-tennantite, and pyrite (Einaudi et al., 2003). Moreover, the presence of carbonate indicates that relatively neutral conditions prevailed at the time of gold deposition.

Thermodynamic modelling suggests that delaying of gold precipitation in late As-rich pyrite III is probably due to these neutral pH conditions generated by interaction with hydrocarbons.

Late gold precipitation may have been triggered by slow cooling in specific favorable sites as fractured anticline hinges, stratigraphic traps or intrusive host rock contacts.

The local occurrence of enargite and traces of digenite as the last sulfide phase having precipitated, together with pyrophyllite, kaolinite and aluminum phosphate–sulfate minerals implies a sudden change of sulfidation state at the final stages of evolution of the system. This conclusion is apparently opposite to the classical view on suggesting an increase in sulfidation degree with time as a result of neutralization and cooling of a magmatic fluid (e.g. Einaudi et al., 2003). However, such a late increase in sulfidation degree Similar observations has been described in other intermediate to low sulfidation epithermal deposits, especially in Mexico, although remaining enigmatic (Camprubi and Albinson, 2007).

Fluid inclusion thermometry and S isotope analyses of pyrite will help to further constrain the gold-bearing fluid origin and physical-chemical characteristics to validate our new model.

Acknowledgements

This research was funded by the Institut Carnot ISIFoR (ORPET project: Systèmes pétroliers aurifères: origine et fonctionnement). The authors would like to thank Tahoe Resources, for logistical and financial support throughout this study, in particular Wilder Garcia, Ricardo Gordillo, Roly Alva and Rene Vilchez.

References

Benavides-Cáceres, V. 1999. Orogenic evolution of the Peruvian Andes: the Andean Cycle. In: Skinner, B.J. (Ed.), Geology and Ore Deposits of the Central Andes. Society of Economic Geologists Special Publication 7, p. 61–107.

Bussey, S., Nelson, E. 2011. Geological analysis of the Shahuindo district, Cajabamba Province, Peru. Prepared by Western Mining Services LLC for Sulliden Gold Corporation.

Camprubí, A., Albinson, T. 2007. Epithermal deposits in México—Update of current knowledge, and an empirical reclassification, in Alaniz-Álvarez, S.A., and Nieto-Samaniego, Á.F., eds., Geology of México: Celebrating the Centenary of the Geological Society of México. Geological Society of America Special Paper 422, p. 377–415, doi: 10.1130/2007.2422(14).

Cline, J.S., Hofstra, A.H., Muntean, J.L., Tosdal, R.M., Hickey, K.A. 2005. Carlin-type gold deposits in Nevada—Critical geologic characteristics and viable models. In Hedenquist, J.W., Thompson, J.H.F., Goldfarb, R.J., and Richards, J.P., eds., Economic Geology 100th Anniversary Volume: Society of Economic Geologists, Littleton, Colorado, p. 451–484.

Defilippi, C.E., Muerhoff, C.V., Williams, T. 2016. Technical Report on the Shahuindo Mine, Cajabamba, Peru. NI 43-101 Technical Report para Tahoe Resources, 307 p.

Einaudi, M.T., Hedenquist, J.W., Inan, E.E. 2003. Sulfidation state of fluids in active and extinct hydrothermal systems: Transitions from porphyry to epithermal environments: Society of Economic Geologists Special Publication 10, p. 285–313.

Eude, A. 2014. La croissance des Andes centrales du nord du Pérou (5-9°S): Propagation d'un prisme orogénique dans un contexte d'héritage tectonique et de subduction plane, PhD Thesis, Toulouse III Paul Sabatier University, France, 323 p.

Fuchs, S. 2016. Metal distribution in pyrobitumen of the Carbon Leader Reef, Witwatersrand Supergroup, South Africa; evidence for liquid hydrocarbon ore fluids. Chemical Geology, v. 426, p. 45-59.

Hodder, R. 2010. The Shahuindo Epithermal Gold Occurrence: Petrographic Reconnaissance & Interpretation of Shape and Size. Cajabamba-Perú. Internal Report for Tahoe Resource. 120 p.

Large, R.R., Bull, S.W., Maslennikov, V.V. 2011. A carbonaceous sedimentary source-rock model for Carlin-type and orogenic gold deposits. Economic Geology, v. 106(3), p. 331-358.

Mégard,F. 1984. The Andean orogenic period and its major structures in central and northern Perú: Journal of the Geological Society of London, v. 141(5), p. 893-900.

Noble D.C, McKee E.H. 1999. The Miocene metallogenic belt of central and northern Perú. In: Skinner BJ (ed) Geology and Ore Deposits of the Central Andes, Society of Economic Geologists Special Publication 7, p. 155-193

Pokrovski G.S., Akinfiev N.N., Borisova A.Y., Zotov A.V., Kouzmanov K. 2014. Gold speciation and transport in geological fluids: insights from experiments and physical-chemical modelling. Geological Society, London, Special Publications, v. 402, p. 9-70.

Pokrovski G.S., Kokh M.A., Guillaume D., Borisova A.Y., Gisquet P., Hazemann J.-L., Lahera E., Del Net W., Proux O., Testemale D., Haigis V., Jonchière R., Seitsonen, A.P., Ferlat G., Vuilleumier R., Saitta A.M., Boiron M.-C., Dubessy J. 2015. Sulfur radical species form gold deposits on Earth. Proceedings of the National Academy of Sciences of the United States of America, v. 112, 13484-13489.

Reich, M,, Kesler, S.E., Utsunomiya S., Palenik, C.S., Chryssoulis, S.L., Ewing. R.C. 2005. Solubility of Gold in Arsenian Pyrite. Geochimica et Cosmochimica Acta, v. 69 (11), p. 2781 2796.

Scherrenberg, A.F., Konh, B.P., Holcombe, R.J., Rosenbaum, G. 2016. Thermotectonic history of the Marañón Fold–Thrust Belt, Peru: Insights into mineralisation in an evolving orogen. Tectonophysics, v. 667, p. 16-36.

Vallance J., Balboa M., Berna B., Cabrera O., Baya C., Baby P., Pokrovski G.S. 2018. Oro y material orgánico en el depósito de Shahuindo (Cajamarca, Peru). Conference abstract. XIX Congreso Peruano de Geología, Lima, Peru. 4 p.

LINKS BETWEEN ORGANIC MATTER AND GOLD-BEARING ARSENIAN PYRITE AT SHAHUINDO (CAJAMARCA, PERU): AN INTEGRATED ANALYTICAL AND MODELING STUDY

Jean Vallance, Macneill Balboa , Brigitte Berna, Omar Cabrera, Camille Baya, Patrice Baby, Gleb S. Pokrovski

NOTAS